PERGAMON

Atmospheric Environment 35 (2001) 2615–2625

ATMOSPHERIC ENVIRONMENT

www.elsevier.com/locate/atmosenv

Determining the sources of atmospheric particles in Shanghai, China, from magnetic and geochemical properties

Jiong Shu[a], John A. Dearing[b], Andrew P. Morse[b,*], Lizhong Yu[a], Nu Yuan[a]

[a]*Department of Geography, East China Normal University, Shanghai 200062, China*
[b]*Department of Geography, University of Liverpool, P.O. Box 147, Liverpool L69 7ZT, UK*

Received 25 January 2000; received in revised form 2 September 2000; accepted 13 September 2000

Abstract

The study describes an investigation into the sources of atmospheric particles collected at 11 sites across Shanghai, China, during one week in November 1998. Source ascription is based on mineral magnetic and geochemical properties, and a chemical mass balance (CMB) model. The CMB model shows that the main contributions to total suspended particles (TSPs) are products of coal combustion, with lesser contributions from construction sites, vehicle emissions, windblown soil and steel-making furnaces. The spatial variability of concentration-dependent magnetic parameters and heavy metal concentrations support the findings from the CMB model. In general, the variability of magnetic quotient parameters is lower than for concentration parameters. This suggests that there are relatively constant proportions of low coercivity 'magnetite' and high coercivity 'haematite' mineral phases in dust samples at all sites, with a dominance of superparamagnetic (SP) and multidomain (MD) + pseudo-single domain (PSD) 'magnetite' grains. MD + PSD grains are produced to a large extent by fossil-fuel combustion emissions, particularly from the main iron and steel manufacturing and power generation industrial complex. Linear multiple regression analyses show that some non-destructive and rapid magnetic measurements may be used to estimate the concentrations of common heavy metals in TSPs.

Keywords: Atmospheric pollution; Environment magnetism; Chemical mass balance; Total suspended particles; Shanghai

1. Introduction

One of the most urgent tasks for atmospheric environmental protection is to monitor present and future particle loadings in urban areas from point and diffuse pollution sources. This allows the drawing-up of policies aimed at reducing emissions and the appraisal of their long-term effectiveness. In many urban areas, the diversity of particle emissions makes source ascription difficult. Organic and inorganic properties of particles are often described using physical and chemical measurements and linked to source properties through chemical mass balance (CMB) receptor models and multivariate models (Henry et al., 1984; Watson et al., 1990; Watson and Chow, 1991; John et al., 1998; Pinto et al., 1998). Increasingly, magnetic properties of particles have also been shown to provide a simple and effective means to source ascription in both modern polluted samples (Hunt et al., 1984; Oldfield et al., 1985; Hunt, 1986; Thompson and Oldfield, 1986; Charlesworth and Lees, 1997; Flanders, 1999; Xie et al., 1999a, b; Matzka and Maher, 1999; Petrovsky and Ellwood, 1999) and pre-industrial sediment (Oldfield et al., 1978). The strong variability of Fe-mineral phases in particles provides the basis for their characterisation from a variety of sources: fossil-fuel combustion, iron and steel manufacturing, plating industries, vehicle emissions, construction materials and wind-blown soil. Previous studies have shown that the magnetic properties of airborne particles may be strongly associated with heavy metal concentrations (Linton et al., 1980; Hunt et al., 1984; Beckwith et al., 1986) and

* Corresponding author.
E-mail addresses: shuj@public4.sta.net.cn (J. Shu), a.p.morse@liv.ac.uk (A.P. Morse).

1352-2310/01/$ - see front matter
PII: S1352-2310(00)00454-4

mutagenic organic compounds (Morris et al., 1995). The legacy of historical particle loadings is often seen in the high concentrations of ferrimagnetic (e.g. magnetite) and canted antiferromagnetic minerals (e.g. haematite) in O and A soil horizons, especially in urban areas and at sites downwind of industrial centres (Strzyszcz, 1989; Dearing et al., 1995; Hay et al., 1997). A major magnetic component consists of Fe-rich spherules ($>10\,\mu m$) in fly-ash (Ondov et al., 1979; Keyser et al., 1978), generated during coal combustion and derived directly from conversion of framboids present in the coal. Hansen et al. (1981) showed that these spherules are enriched with chromium, manganese, cobalt, nickel, copper, zinc and beryllium. Strong associations between magnetic parameters and the metal contaminants, but not total Fe, suggest that most Fe exists in weakly magnetic forms, which in mixtures of particles may provide evidence for minerals with natural origins, such as soil (Georgeaud et al., 1997). In a recent pilot study of atmospheric particles in Shanghai, China, magnetic measurements alone provided an exceptionally simple and effective approach for identifying daily variations in particle loading and sources (Shu et al., 2000). The purpose of this paper extends the analysis of these samples to investigate the value and sensitivity of magnetic techniques in combination with heavy metal analyses. Receptor modelling calculations are used to define types and proportions of source particles in TSPs deposited in residential areas and urban districts at various distances from two large industrial complexes. These districts were selected for this study because local residents may already be exposed to high TSP loadings, particularly from coal-burning and re-worked road dust (Ji et al., 1993) under certain weather conditions. For example, during autumn 1996, daily TSP concentrations reached $264\,\mu g\,m^{-3}$ in the Shanghai metropolitan area, a value that was $23\,\mu g\,m^{-3}$ higher than the annual mean value, and $38\,\mu g\,m^{-3}$ higher than the rural area during the same period (Shanghai Municipal Environmental Protection Bureau, 1997).

2. Sample collection and measurements

2.1. Sample collection

TSPs were sampled at 11 sites during the period 5th to 11th November 1998, mainly within and around Taopu, the chemical industrial area (sites 1, 2, 4) lying at the NW edge of the city centre, and Baoshan, the iron and steel manufacturing and coal-fired power generation complex plants (sites 6, 7, 8, 9, 10, 11) lying N of the city area, (Fig. 1). Two further sampling sites were situated in residential areas, about 2.5 km W (site 3) and 5 km S (site 5) of the Taopu area (Fig. 1). An automatic meteorological station, made by DAVIS Instruments Corp. USA, stationed close to site 11 provided standard meteorological data adjusted with records from the city's meteorological observatory. TSPs were collected in mid-volume samplers manufactured by Shanghai Hongyu Equipment Factory (Ji et al., 1993) that were placed on roofs and canopies at least 3 m above the ground surface. The samplers were continuously operated for 24 h period per sample, at a flow rate of $0.15\,m^3\,min^{-1}$. The sampling program gave 75 filters with TSP samples (site 5 was short of two days sampling). Clean and pre-weighed glass fibre filters (diameter 100 mm) were stored in a desiccator for 24 h before loading into sample holders. The filters with samples were stored in a desiccator for 24 h again after sampling and mass calculated from weight difference.

2.2. Magnetic and metal measurements

Routine isothermal magnetic measurements (Thompson and Oldfield, 1986; Walden et al., 1999; Maher and Thompson, 1999) were carried out on filters folded into 10 ml plastic pots. Low- and high-field magnetic susceptibility (χ_{LF} and $\chi_{HF}\,10^{-8}\,m^3\,kg^{-1}$) and derived frequency-dependent susceptibility (χ_{FD} $10^{-8}\,m^3\,kg^{-1}$) measurements were obtained using a dual-frequency (470 and 4700 Hz) Bartington Instruments MS2 Susceptibility Meter. Anhysteretic remanent magnetisation (ARM $10^{-5} m^3\,kg^{-1}$) was induced in a steady field of 0.1 mT imposed on a peak AF field of 100 mT, and the remanence measured in a Molspin spinner magnetometer. The values are expressed as susceptibility of ARM (χ_{ARM} 10^{-8} $m^3\,kg^{-1}$) by dividing ARM by the steady field. Acquisition of isothermal remanent magnetisation (IRM $10^{-5} Am^2\,kg^{-1}$) was made in fields of 20, 30 mT, 1 T (SIRM) followed by demagnetisation in -20, -30, -40, -50, -100, and -300 mT using a Molspin pulse magnetiser and spinner magnetometer. Magnetic parameters are expressed on both mass-specific and quotient bases in order to give quantitative and qualitative information χ_{LF} ($10^{-8}\,m^3\,kg^{-1}$); χ_{FD} ($\chi_{LF} - \chi_{HF}$ $10^{-8}\,m^3\,kg^{-1}$); SIRM ($10^{-5}\,Am^2\,kg^{-1}$); χ_{ARM} ($10^{-8} m^3\,kg^{-1}$); SOFT (SIRM $-$ IRM$_{-20mT}$ $10^{-5} Am^2\,kg^{-1}$); HIRM ([SIRM $-$ IRM$_{-300mT}$]/2 $10^{-5} Am^2\,kg^{-1}$); χ_{FD}% ($100\times[\chi_{LF-}\chi_{HF}]/\chi_{LF}$); SIRM/$\chi_{LF}$ ($kA\,m^{-1}$); SOFT % ($100\times$[SOFT/SIRM]) and HARD % (100*[HIRM/SIRM]). The magnetic susceptibility χ_{LF} represents the total contribution of Fe-bearing minerals in the mineral assemblage but is normally controlled by the total ferrimagnetic concentration (Thompson and Oldfield, 1986). Frequency-dependent susceptibility χ_{FD} approximates to the total concentration of superparamagnetic (SP) grains (Dearing et al., 1996), while ARM (χ_{ARM}) approximates to the concentration of stable single domain (SSD) and fine pseudo-single domain (PSD) ferrimagnetic grains (King et al., 1982; Maher, 1988). Saturation isothermal remanent magnetisation (SIRM) is related to the total remanence carrying mineral

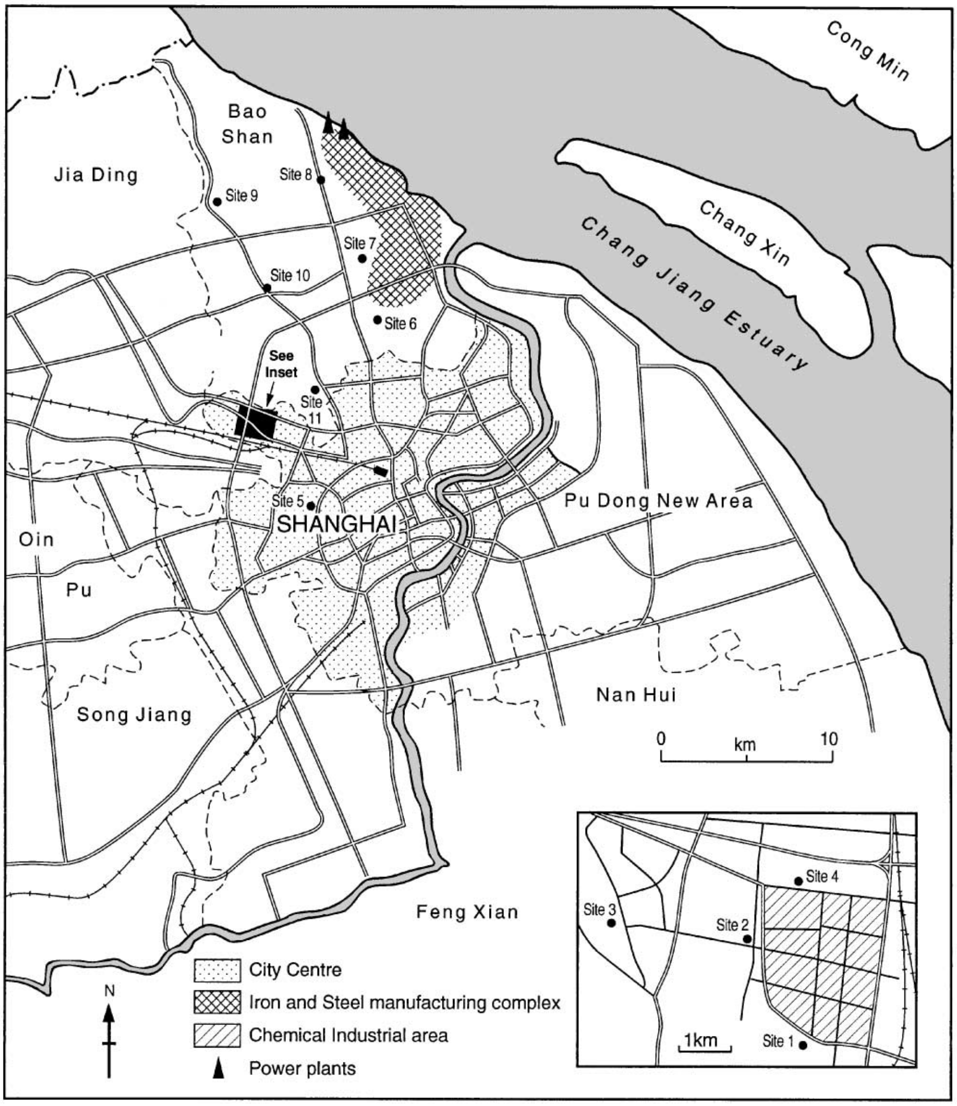

Fig. 1. Shanghai, China. The location of 11 sampling sites around two industrial complexes.

assemblage but controlled largely by SSD ferrimagnetic grain concentrations and the presence of canted antiferromagnetic minerals. Thompson's calculation (1986) suggested that low coercivity remanence (SOFT) is expected to approximate to the concentration of 'magnetite', especially for low coercivity grains in the multidomain (MD) and possibly SP/SSD boundary ranges, while Oldfield and Richardson (1990) suggest that high coercivity remanence (HIRM) can be used to estimate the total concentration of canted antiferromagnetic minerals ('haematite'). SOFT % and HARD % can be used to approximate the relative proportion of ferrimagnetic and canted antiferromagnetic components in a sample, respectively (Oldfield, 1991). SIRM/χ_{LF} is controlled by SSD magnetite grains and to a lesser extent by the proportion of 'haematite'. χ_{FD}% is related to the proportions of SP magnetite and may be interpreted semi-quantitatively (Dearing et al., 1997).

Dust samples were digested in hydrofluoric acid, nitric acid and perchloric acid in platinum crucibles (Thompson and Walsh, 1991a) and metal concentrations for 14 elements (Na, Mg, Al, K, Ca, Ti, Fe, Cu, Pb, Zn, Mn, Ni, V, As) were determined (Thompson and Walsh, 1991b) by ICPS (Perkin-Elmer Plasma-2000). The standard deviation of repeated measurements was $<10\%$ for all samples. The arithmetical mean of metal concentrations of 10 clean filters was measured and subtracted from measurements of filters with samples.

Table 1

Magnetic measurements of TSPs from 75 samples at different sites

(A) Chemical industrial area (Taopu) and residential quarters

	Site 1			Site 2			Site 3			Site 4			Site 5		
	Range	Mean	SD	Range	Mean	SD	Range	Mean	SD	Range	Mean	SD	Range	Mean	SD
χ_{LF} [a]	285.6–734.4	493.5	167.5	217.4–627.9	408.5	145.2	213.2–444.9	298.7	72.4	247.0–840.4	523.7	222.7	279.3–601.4	413.2	112.1
χ_{FD} [b]	20.1–50.0	35.8	9.5	15.2–44.2	28.4	9.3	17.4–30.4	23.4	5.8	17.0–56.3	36.3	13.9	3.1–66.2	22.8	22.7
χ_{FD} %	5.4–11.1	7.5	1.7	5.9–8.8	7.1	0.8	6.8–12.7	8.0	1.9	6.3–8.7	7.1	0.7	1.1–11.0	4.6	3.4
SIRM [c]	3782.1–9727.8	6660.5	2063.1	2899.7–9645.1	5729.5	2160.6	3428.1–6208.6	4389.0	944.4	3323.2–12889.7	7294.8	3069.7	3282.9–6987.2	5090.7	1270.0
χ_{ARM} [d]	38.2–1091.0	440.9	332.9	69.6–750.2	298.6	228.4	37.4–439.2	219.4	153.2	90.6–1051.0	403.0	326.0	49.8–479.0	274.3	188.6
SIRM/χ_{LF} [e]	12.6–14.7	13.6	0.6	12.9–15.4	14.0	0.9	13.3–16.3	14.8	1.1	10.9–19.1	14.2	2.7	10.8–12.7	12.4	1.6
HIRM [f]	109.9–447.6	269.8	118.8	140.9–805.4	313.0	222.4	95.5–414.6	254.4	114.4	169.7–1642.0	406.7	504.9	131.9–569.0	298.6	164.2
HARD %	2.2–6.7	4.1	1.4	2.2–8.6	5.4	2.5	2.2–10.0	6.2	3.5	2.0–12.7	4.9	3.5	2.6–9.7	6.1	3.1
SOFT [g]	1253.5–2677.8	1801.7	480.7	808.1–2384.0	1484.4	555.6	810.1–1452.6	1168.0	232.4	994.4–3339.2	1824.7	835.3	853.8–2075.6	1463.4	465.7
SOFT %	22.9–40.7	28.0	5.8	22.8–28.3	26.0	1.8	23.4–35.4	26.9	3.8	19.8–29.9	24.9	3.4	25.5–35.6	28.4	3.7

(B) Iron and steel manufacturing and power generation complex (Baoshan)

	Site 6			Site 7			Site 8			Site 9			Site 10			Site 11		
	Range	Mean	SD	Range	Mean	SD	Range	Mean	SD	Range	Mean	SD	Range	Mean	SD	Range	Mean	SD
χ_{LF} [a]	538.8–2852.5	1521.3	925.6	336.0–1320.8	743.1	304.5	294.6–1708.1	1098.1	454.2	248.9–749.2	410.3	164.6	209.6–627.1	441.1	120.2	229.5–441.7	327.8	77.9
χ_{FD} [b]	8.7–38.4	23.6	10.7	16.7–89.3	36.5	24.7	20.3–118.8	66.0	28.9	20.0–35.9	26.3	5.1	14.9–45.2	31.8	8.3	10.8–37.0	22.3	8.3
χ_{FD}%	0.4–5.2	2.3	1.8	1.4–8.8	5.2	2.7	4.5–7.0	6.1	0.9	4.0–8.0	7.0	1.8	4.9–12.7	7.5	2.3	3.8–10.7	6.8	2.0
SIRM [c]	7163.6–54882.7	22087.0	15958.2	4334.0–17245.5	11174.5	4387.7	4591.9–23861.6	15332.3	6129.5	3520.6–16244.4	6669.8	4396.8	2772.6–10877.9	7006.2	2476.8	3052.5–7659.9	4977.8	1430.8
χ_{ARM} [d]	39.3–3510.0	1454.0	1196.3	41.4–1328.2	605.4	427.4	102.9–1910.4	949.2	612.8	34.5–496.6	347.9	193.4	48.2–616.3	379.6	195.0	45.8–533.5	314.6	182.3
SIRM/χ_{LF} [e]	12.1–19.2	14.2	2.3	12.2–18.4	15.1	2.0	12.9–16.5	14.2	1.3	10.6–21.7	15.1	3.5	12.0–20.7	15.6	2.7	13.3–17.3	15.1	1.5
HIRM [f]	244.9–8574.7	1731.8	2806.0	182.0–1382.8	448.6	389.4	234.6–1110.7	646.0	254.3	125.4–498.2	252.3	128.9	211.5–726.1	418.4	188.7	102.2–273.2	216.2	55.7
HARD%	2.6–15.6	5.7	4.6	1.8–9.8	4.1	2.7	3.0–6.0	4.4	0.9	3.1–5.6	4.0	0.8	3.9–8.6	6.1	1.7	3.1-6.7	4.4	1.1
SOFT [g]	2138.3–14945.3	6162.1	4421.6	1277.8–4497.6	2943.2	1191.2	1674.0–7683.2	4233.1	1872.3	1011.6–2731.9	1673.0	647.4	920.0–2802.6	1770.2	536.1	786.4–1950.5	1346.6	392.7
SOFT%	23.5–32.4	27.7	2.6	20.6–29.8	26.4	3.1	20.3–36.5	28.3	4.7	16.8–38.6	28.4	6.7	18.1–37.9	26.8	6.9	20.4–42.2	27.7	6.7

[a] $10^{-8}\,m\,kg^{-1}$.

[b] $10^{-8}\,m^3\,kg^{-1}$.

[c] $10^{-5}\,Am^2\,kg^{-1}$.

[d] $10^{-8}\,m^3\,kg^{-1}$.

[e] $kA\,m^{-1}$.

[f] $10^{-5}\,Am^2\,kg^{-1}$.

[g] $10^{-5}\,Am^2\,kg^{-1}$.

Mean in the table above: Arithmetical mean.

3. Results and discussions

3.1. TSP concentrations

The wind speeds were relatively weak (0.2–0.6 $\mathrm{m\,s^{-1}}$) during the sampling period and northerly, except for a southerly wind on the fifth day. Therefore, it is assumed that long-distance transported particles are less significant than local pollution sources over the period. Overall, the spatial distribution of TSPs shows that the mean dust concentrations at site 6 (533.1 $\mu\mathrm{g\,m^{-3}}$) and site 7 (398.8 $\mu\mathrm{g\,m^{-3}}$) close to Baoshan and at a downwind location (site 11 537.0 $\mu\mathrm{g\,m^{-3}}$) were higher than that at site 1 (233.5 $\mu\mathrm{g\,m^{-3}}$), site 2 (269.2 $\mu\mathrm{g\,m^{-3}}$) and site 4 (273.8 $\mu\mathrm{g\,m^{-3}}$) adjacent to Taopu. Highest concentrations (1069.4 $\mu\mathrm{g\,m^{-3}}$) were attained on one day at site 5. TSP concentrations for all sites are higher with NW winds and lower with S wind directions, implying the important contribution of emissions from the northern industrial zone.

3.2. Magnetic properties of TSPs

The mean magnetic measurements of 10 clean filters for χ_{LF}, SIRM and χ_{ARM} are 2.3753 ± 0.2401 ($10^{-8}\mathrm{m^3\,kg^{-1}}$), 7.0376 ± 0.3002 ($10^{-5}\mathrm{Am^2\,kg^{-1}}$) and 0.4614 ± 0.1107 ($10^{-5}\mathrm{m^3\,kg^{-1}}$) respectively, and while the values show some Fe contamination during manufacture they are typically 2–3 orders of magnitude lower than measurements made on filter plus dust samples. Table 1 summarizes the ranges, arithmetic means and standard deviations of magnetic measurements of daily TSP samples, showing that the magnetic concentrations, minerals and grain sizes vary from site-to-site and day-to-day. The highest maximum and mean magnetic concentrations (χ_{LF}, SIRM, χ_{ARM}, HIRM and SOFT) are found at sites 6, 7 and 8 (Table 1) adjacent to the Baoshan complex (Fig. 1). These data are explained by the widespread coexistence of ferrimagnetic 'magnetite' phases in SSD, PSD and MD sizes, and high coercivity 'haematite' phases. The exact mineralogy is likely to be complex and non-stoichiometric. Maximum, minimum and mean χ_{LF} and SIRM values for the other sites are 20–60% lower. The lowest magnetic concentrations are found at site 3, a residential quarter $\sim$3 km W of the Taopu chemical industrial zone. The *t*-test results (Table 2) indicate that the high values of χ_{LF} and SIRM at sites 6, 7 and 8 are statistically distinct from other sites, demonstrating the effect of the Baoshan complex as a major source of non-SP 'magnetite' to local and downwind locations. In contrast, the influence of the Taopu industrial zone on dust magnetic properties seems slight. These tendencies

Table 2
Probability by *t*-test from 75 samples at 11 sites with χ_{LF} (A) and SIRM (B). Bold script means to reject the null hypothesis (Expectations are equal) at the 0.05 significance level

(A) χ_{LF} Site	2	3	4	5	6	7	8	9	10	11
1	0.3662	**0.0226**	0.7951	0.4140	**0.0202**	0.1040	**0.0099**	0.4025	0.5451	**0.0483**
2		0.1232	0.3094	0.9575	**0.0131**	**0.0318**	**0.0041**	0.9844	0.6796	0.2533
3			**0.0364**	0.0785	**0.0073**	**0.0046**	**0.0011**	0.1542	0.0286	0.5149
4				0.3730	**0.0247**	0.1798	**0.0166**	0.3355	0.4394	0.0646
5					**0.0354**	**0.0345**	**0.0130**	0.9762	0.7172	0.1858
6						0.0741	0.3346	**0.0135**	**0.0150**	**0.0084**
7							0.1377	**0.0364**	**0.0432**	**0.0071**
8								**0.0045**	**0.0050**	**0.0015**
9									0.7178	0.2887
10										0.0765
(B) SIRM										
1	0.4600	**0.0305**	0.6818	0.1983	**0.0368**	**0.0416**	**0.0065**	0.9963	0.7972	0.1266
2		0.1890	0.3272	0.6007	**0.0285**	**0.0184**	**0.0035**	0.6467	0.3602	0.4910
3			**0.0467**	0.3400	**0.0189**	**0.0030**	**0.0010**	0.2379	0.0324	0.4166
4				0.1966	**0.0456**	0.1013	**0.0140**	0.7801	0.8607	0.1196
5					**0.0553**	**0.0205**	**0.0072**	0.4926	0.1781	0.9000
6						0.1323	0.3522	**0.0416**	**0.0411**	**0.0266**
7							0.2016	0.1010	**0.0328**	**0.0065**
8								**0.0157**	**0.0095**	**0.0017**
9									0.8730	0.3877
10										0.1080

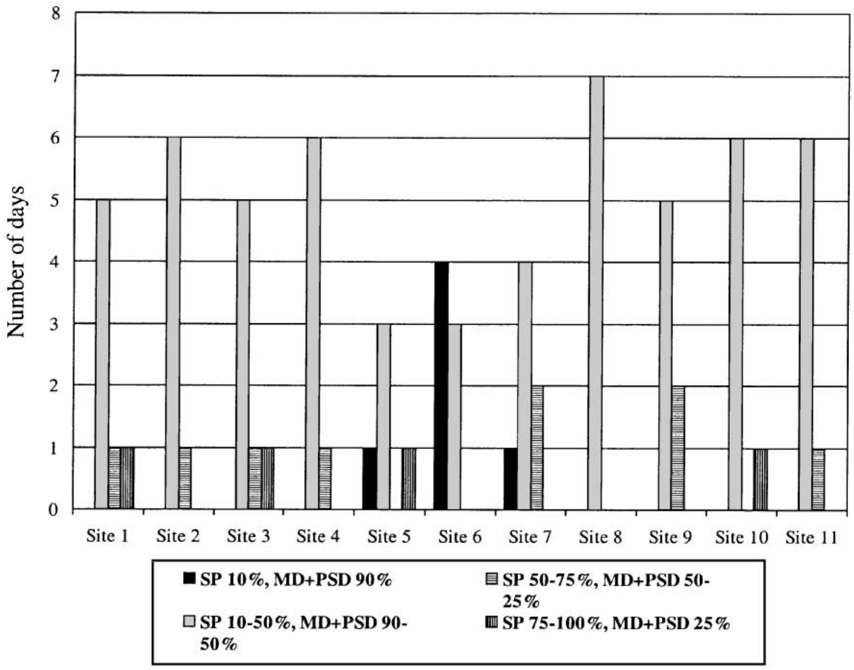

Fig. 2. Number of days dominated by SP and MD + PSD magnetic domain sizes at 11 sites during sampling period.

in mean data are apparent even when the day-to-day magnetic variability is taken into account (Table 1) (Shu et al., 2000).

Variability in magnetic quotients is generally less than for concentration parameters. The small ranges of mean values of SOFT% (24–28%), HARD% (4–6%) and SIRM/χ_{LF} (12–16 kA m^{-1}) across the sites suggest relatively constant proportions of 'magnetite' and 'haematite' mineral phases at all sites. Mean values for frequency-dependent susceptibility percent (χ_{FD}%) > 7 % at sites 1, 2, 3, 4, 9 and 10 indicate a significant contribution by ultra fine-grained ($<0.03\,\mu$m) SP 'magnetite', typically found in soil. According to a semi-quantitative mixing model (Dearing et al., 1997) the proportion of grain sizes is typically 10–50% SP and 50–90 % MD + PSD at all sites during most of the sampling period (Fig. 2). However, the proportion of MD + PSD grains rises to 90% on 1 and 4 days at sites 6 and 7, respectively, both situated closest to the Baoshan iron and steel complex. The effect of Baoshan may also be apparent at site 5, which although 13 km downwind, has an enhanced proportion of MD + PSD grains. Iron and steel manufacturing, fossil-fuel combustion and associated traffic activity clearly give rise to ferrimagnetic (and ferromagnetic) phases in fly-ash and Fe-particles dominated by MD + PSD domain sizes, but it is not possible to distinguish between them using these magnetic measurements alone (Petrovsky and Ellwood, 1999).

3.3. Distribution of heavy metal and magnetic concentrations

Fig. 3 gives arithmetic mean measurements of 14 chemical elements and 3 magnetic parameters (χ_{LF}, SIRM, and χ_{FD}) for the sampled particles. The concentrations of some marker elements Fe, Mn, Zn and Ni for steel-making furnaces (Xudong et al., 1994; Institute of Environmental Protection and Research in Shanghai, 1996; Zhang et al., 1998) at sites close to Baoshan (sites 6 and 8) are higher than at other sites. The effect of these industries as a source for Fe is also seen in the downwind site 5. The high concentrations of marker elements Al, Ti and As at sites 1, 4, 8 and 10 indicate a predominant coal combustion source (Xudong et al., 1994; Institute of Environmental Protection and Research in Shanghai, 1996; Zhang et al., 1998), whereas Ca, Mg and Mn indicate construction materials, and Al, K, Ti and Mn indicate wind-blown soil. Higher concentrations of Pb at sites 3 and 8 reflect the impact of vehicle emissions. The χ_{LF} and SIRM values have similar patterns as Fe, Mn, Ni, V and Zn confirming that ferrous particles and magnetic spherules in emissions from heavy industry and coal-fired power generation are the main causes of high ferrimagnetic concentrations. The association of χ_{FD} with Al, As, Cu, Mg and Na is consistent with soil and other lithogenic sources for the SP grain fraction.

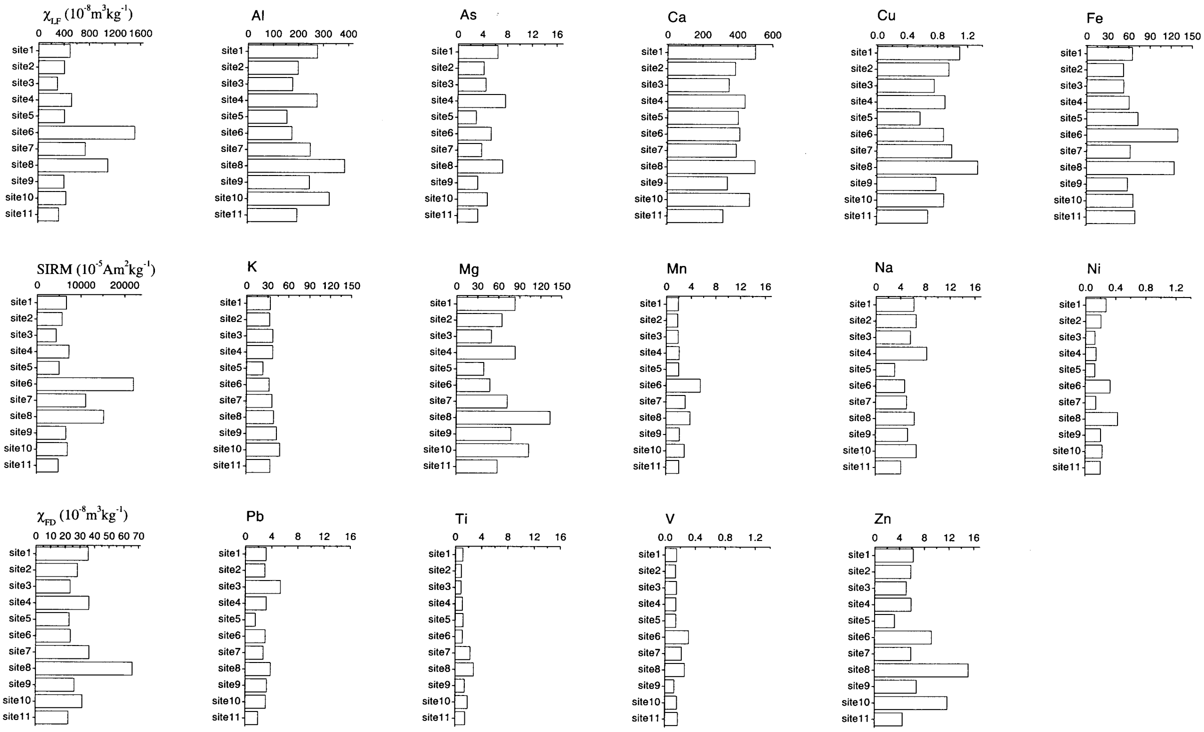

Fig. 3. The mean concentrations (mg g^{-1}) of 14 elements and 3 magnetic parameters for TSPs at 11 sites.

Table 3
Source profile (arithmetic mean values) used in modelling calculations (Units: mg g^{-1})

Source types	Na	Mg	Al	K	Ca	Ti	Fe	Cu	Pb	Zn	Mn	Ni	V	As
Coal combustion	4.99	1.56	90.90	4.45	8.31	4.10	9.16	0.53	1.88	2.46	0.12	0.10	0.10	0.20
Vehicle emissions	4.04	6.49	25.10	6.29	58.59	1.60	19.71	0.52	6.40	1.27	0.62	0.10	0.10	0.10
Steel-making furnace	9.25	49.32	6.78	6.89	53.50	0.90	242.4	0.96	3.63	19.04	27.10	24.00	0.10	0.10
Cement	0.74	23.00	51.50	4.40	3560	3.20	22.68	0.08	0.28	0.40	1.39	0.20	0.10	0.10
Soil	9.32	1.21	79.40	23.40	9.87	5.20	40.88	0.08	0.28	0.40	1.08	0.20	0.10	0.10
Oil boiler	17.50	5.15	0.00	0.37	36.27	0.60	5.65	13.42	0.15	0.51	0.47	8.40	1.00	0.00

3.4. Chemical mass balance calculations

Estimates of the contributions of sourced particles to the TSPs at all sites were made using a chemical mass balance (CMB 7.0 US Environmental Protection Agency) receptor model (Watson et al., 1990; Watson and Chow, 1991). The CMB analysis consists of an effective variance least-squares estimation of a set of linear equations:

$$\mathrm{ME}_i = \sum_{j=1}^{J} F_{ij} S_j, i = 1, \ldots, I \tag{1}$$

where ME is the concentration of elements i in TSPs measured at 11 sites; F is the fraction of elements i in TSP emissions from sources j, I is the number of chemical elements, and S_j are estimations of the contribution of source j (Watson et al., 1990). In Shanghai, six main source-types (j) are officially defined according to the published associations between chemical elements (i) for coal combustion, vehicle emissions, oil boiler combustion, steel-making furnaces, cement production and wind-blown soil (Xudong et al., 1994; Institute of Environmental Protection and Research in Shanghai, 1996; Zhang et al., 1998). The source composition profiles (F) with 14 (I) marker elements (i) for six emission sources (j) that are used in the receptor modelling calculations are listed in Table 3.

The CMB modelling results for mean primary constituents of 75 samples for each sampling site are shown

Table 4
Relative arithmetic mean contributions of different source types to TSPs

(A) Chemical industrial area (Taopu) and Residential quarters

Source types	Site 1	Site 2	Site 3	Site 4	Site 5
Coal combustion	0.509	0.232	0.394	0.545	0.312
Vehicle emissions	0.199	0.354	0.298	0.186	0.106
Steel-making furnace	0.014	0.000	0.005	0.003	0.026
Cement	0.274	0.247	0.269	0.266	0.454
Soil	0.000	0.167	0.034	0.000	0.102
Oil boiler	0.000	0.000	0.000	0.000	0.000
χ^2	1.9	2.0	1.7	1.9	1.8

(B) Iron and steel manufacturing and power generation complex (Baoshan)

Source types	Site 6	Site 7	Site 8	Site 9	Site 10	Site 11
Coal combustion	0.196	0.201	0.601	0.408	0.529	0.415
Vehicle emissions	0.056	0.347	0.157	0.459	0.260	0.186
Steel-making furnace	0.095	0.028	0.047	0.020	0.006	0.027
Cement	0.374	0.201	0.195	0.061	0.204	0.250
Soil	0.279	0.222	0.000	0.051	0.000	0.122
Oil boiler	0.000	0.000	0.000	0.000	0.000	0.000
χ^2	1.4	1.8	1.5	2.0	2.1	1.8

in Table 4. Also shown are measures of the CMB model accuracy, given by χ^2 ($p = 0.01$). Values of χ^2 lie in the range 1.4–2.0, indicating an acceptable fit of the model to the data (Watson et al., 1990). It can be seen that coal combustion constitutes the main source of TSPs, such as site 1 (51%) situated downwind of Taopu; site 10 (53%), site 11 (42%) and site 4 (55%) situated downwind of Baoshan. At site 8, close to the Baoshan power plants the contribution by particles from coal combustion rises to $\sim 60\%$. Despite the introduction of some new power generation technologies, the data suggest that older coal-fired combustion processes still represent the major pollution source at many sites across the city. Emissions from vehicles and cement production, which are dependent on local traffic distributions, road conditions and urban construction, are the next ranked sources of TSPs. The contribution by particles from vehicle emissions reaches $\sim 30\%$ at site 3, $\sim 35\%$ at site 2 and site 7, and $\sim 46\%$ at site 9. The particle contribution from cement production is ~ 25–27% at most sites, comparable to values of $\sim 20\%$ measured in Beijing, China (Wang, 1985), which rise to over 35 % at sites 5 and 6 adjacent to construction sites. These high values demonstrate the significance of dust emissions related to the widespread construction activities in this rapidly developing city. On average, steel-making emissions appear to make relatively small contributions to TSPs ($< 10\%$), even at sites in proximity to furnaces (sites 6, 7 and 8).

3.5. Elemental-magnetic relationships

The first transition group elements (V, Cr, Mn, Fe, Co, Ni, Cu and Zn) are enriched in the magnetic spinel fraction of fly-ash (Hulett et al., 1980). Thus this group is expected to be associated with χ_{LF}, SIRM, χ_{ARM}, SOFT and HIRM values. In contrast, s-block elements such as Na and K in group I, Mg and Ca in group II and p-block elements such as Al in group III, and As in group V elements are mostly enriched in soil and construction materials, and are expected to be associated with χ_{FD} and HIRM values. These associations in the present data set are shown by multiple linear regression equations

$$X_{\mathrm{TRANSITION}} = \alpha_1 \chi_{\mathrm{LF}} + \alpha_2 \mathrm{SIRM} + \alpha_3 \chi \mathrm{ARM} + \alpha_4 SOFT + \alpha_5 HIRM, \quad (2)$$

$$Y_{\mathrm{GROUPI\text{–}V}} = \beta_1 \chi_{\mathrm{FD}} + \beta_2 \chi_{\mathrm{HIGH}} + \beta_3 \mathrm{HIRM}. \quad (3)$$

Here $X_{\mathrm{TRANSITION}}$ and $Y_{\mathrm{GROUP\ I\text{–}V}}$ represent first transition group elements and group I–V elements, respectively, and α_i, β_j (i from 1 to 5, j from 1 to 3) are partial regression coefficients. Using the stepwise method, from Eq. (2) and (3), we obtain regression equations for 11 elements (Table 5) showing relatively high correlation coefficients ($R^2 = 0.50$–0.94; $p = 0.01$) with corresponding magnetic parameters. Relationships between magnetic parameters and K, Ti and Pb are statistically insignificant. The overall findings show that (1) the

Table 5
Linear multiple regression of magnetic parameters with chemical elements in 75 TSP samples

R square	*F*	Signif. *F*	Regression equations
			First transition elements
0.9420	235.5970	0.0000	$Fe = 23.6756 + 0.1578\ \chi_{LF} - 0.0041$ SIRM
0.6125	20.0087	0.0000	$Zn = 4.1001 + 0.0059\ \chi_{LF}$
0.7179	76.3290	0.0000	$V = 0.0986 + 0.015\ \chi_{LF}$
0.8594	183.4290	0.0000	$Mn = 1.1572 + 0.0002$ SIRM
0.6289	24.5700	0.0000	$Ni = 0.0938 + 0.0003\ \chi_{LF} - 0.0001$ HIRM
0.5001	13.4390	0.0001	$Cu = 0.6200 + 0.0008\ \chi_{LF} - 0.0002$ HIRM
			Elements in group I and II
0.6279	24.4636	0.0000	$Ca = 190.6098 + 7.2344\ \chi_{FD} + 0.0514$ HIRM
0.6451	16.9624	0.0000	$Na = 1.2181 + 0.2178\ \chi_{FD} + 0.0040$ HIRM $- 0.0019$ SOFT
0.5400	10.9539	0.0001	$Mg = 29.8486 + 1.7123\ \chi_{FD} + 0.0146$ HIRM $- 0.0055$ SOFT
			Elements in group III and V
0.6628	28.5053	0.0000	$Al = 82.7519 + 5.3494\ \chi_{FD} + 0.0241$HIRM
0.6113	14.6752	0.0000	$As = 0.4250 + 0.1442\ \chi_{FD} + 0.0026$ HIRM $- 0.0051\ \chi_{ARM}$

first transition group elements V, Mn, Fe, Ni and Zn are enriched in the magnetite component (χ_{LF} and SIRM) that is derived mainly from coal-fired combustion processes; (2) the relationships between the elements Ca, Na, Mg, Al and As, and HIRM and χ_{FD}, indicate that the main sources of 'haematite' phases are wind-blown soil and construction materials carrying particles containing $CaCO_3$, Al-compounds and Mg-compounds. Both results are consistent with the source apportionment derived from CMB modelling and confirm that magnetic parameters may be used to identify dust sources and as proxies for the concentration of chemical elements.

4. Conclusions

- The spatial and temporal distributions of TSP loadings and their magnetic properties sampled during one week at 11 sites across Shanghai, China are predominantly related to particles emitted from the northern Baoshan industrial and power station complex.
- Particles from other sources (wind-blown road dust, soil and other emissions) comprise secondary components that become relatively more important with distance away from the northern industrial zone and urban area.
- These findings are supported by the outputs from a chemical mass balance receptor model that apportions particles to iron and steel manufacturing, power generation, vehicle emissions, oil boilers, construction and wind-blown soils using 14 marker elements. Coal combustion from all sources constitutes the main source of TSPs, with particles from construction materials, vehicles, wind-blown soil and steel making furnaces ranked lower.
- Linear regression equations with heavy metal and magnetic parameters reveal that χ_{LF}, SIRM, HIRM, SOFT, χ_{ARM} and χ_{FD} may be used to estimate the concentrations of the main metal elements of TSPs from anthropogenic sources.
- The results show that a combined magnetic and geochemical characterization of TSPs in urban and industrial settings may mutually reinforce source definition. Rapid and non-destructive magnetic measurements provide a very useful method for making first order estimations of TSP sources and heavy metal contamination.

Acknowledgements

We gratefully acknowledge financial support by the National Natural Science Foundation of China (Project Approval No. 49671069) and the University of Liverpool. Mr. Bob Jude provided valuable help with magnetic experiments. ICPS analyses were made at The State Key Laboratory of East China Normal University under the direction of Prof. Sun Zhenbin. Mr. Baogeng He, Mr. Liantang Den, Mr. Tianhan Jiang and Mr. Xiaomin Yang kindly provided the particle samples. Drs. S.J. Sangode, Yuquan Hu and Prof. Chaoyi Li, and two anonymous reviewers provided useful comments on the work. We thank Mrs. Sandra Mather for the cartography.

References

Beckwith, P.R., Ellis, J.B., Revitt, D.M., 1986. Heavy metal and magnetic relationships for urban source sediments. Physics of the Earth and Planetary Interiors 42, 67–75.

Charlesworth, S.M., Lees, J.A., 1997. The use of mineral magnetic measurements in polluted urban lakes and deposited dusts, Coventry, U.K. Physics and Chemistry of the Earth 22, 203–206.

Dearing, J.A., Bird, P.M., Dann, R.J.L., Benjamin, S.F., 1997. Secondary ferrimagnetic minerals in Welsh soils: a comparison of mineral magnetic detection methods and implications for mineral formation. Geophysical Journal International 120, 727–736.

Dearing, J.A., Dann, R.J.L., Hay, K., Lees, J.A., Loveland, P.J., Maher, B.A., O'Grady, K., 1996. Frequency-dependent susceptibility measurements of environmental materials. Geophysical Journal International 124, 228–240.

Dearing, J.A., Lees, J.A., White, C., 1995. Mineral magnetic properties of acid gleyed soils under oak and Corsican pine. Geoderma 68, 309–319.

Flanders, P.J., 1999. Identifying fly ash at a distance from fossil fuel power stations. Environmental Science and Technology 33, 528–532.

Georgeaud, V.M., Rochette, P., Ambrosi, J.P., Vandamme, D., Williamson, D., 1997. Relationship between heavy metals and magnetic properties in a large polluted catchment: the Etang de Berre (South of France). Physics and Chemistry of the Earth 22, 211–214.

Hansen, L.D., Siberman, D., Fisher, G.L., 1981. Crystalline components of stack-collected, size-fractionated coal fly ash. Environmental Science and Technology 15, 1057–1062.

Hay, K.L., Dearing, J.A., Baban, S.M.J., Loveland, P., 1997. A preliminary attempt to identify atmospherically-derived pollution particles in English topsoils from magnetic susceptibility measurements. Physics and Chemistry of the Earth 22, 207–210.

Henry, R.C., Lewis, C.W., Hopke, P.K., 1984. Review of receptor model fundamentals. Atmospheric Environment 18, 1507–1515.

Hulett, L.D., Weinberger, A.J., Northcutt, K.J., Ferguson, M., 1980. Chemical species in fly ash from coal-burning power plants. Science 210, 1356–1358.

Hunt, A., 1986. The application of mineral magnetic methods to atmospheric aerosol discrimination. Physics of the Earth and Planetary Interiors 42, 10–21.

Hunt, A., Jones, J., Oldfield, F., 1984. Magnetic measurements and heavy metals in atmospheric particles of anthropogenic origin. The Science of the Total Environment 33, 129–139.

Institute of Environmental Protection and Reseach in Shanghai, 1996. Impact of TSPs on the atmospheric environment and its reduction project in Shanghai. Unpublished Report.

Ji, X., Jiang, D., Fei, S., Yuan, H., He, P., Ye, B., Lei, Z., Feng, C., 1993. Road dust emission inventory for the metropolitan area of Shanghai city. Atmospheric Environment 27A, 1735–1741.

John, L.A., Willis, R.D., Buckley, T.J., Chow, J.C., Watson, J.G., Rhoads, G.G., Lioy, P.J., 1998. Chemical mass balance source apportionment of lead in house dust. Environmental Science and Technology 32, 108–114.

Keyser, T.R., Natusch, D.F.S., Evans, C.A., Linton, R.W., 1978. Characterizing the surfaces of environmental particles. Environmental Science and Technology 12, 768–773.

King, J., Banerjee, S.K., Marvin, J., Özdemir, Ö., 1982. A comparison of different magnetic methods for determining the relative grain size of magnetite in natural materials: some results from lake sediments. Earth and Planetary Science Letters 59, 404–419.

Linton, R.W., Natusch, R.L., Soloman, R.L., Evans Jr., C.A., 1980. Physio-chemical characterization of lead in urban dusts. A microanalytical approach to lead tracing. Environmental Science and Technology 9, 227–230.

Maher, B.A., 1988. Magnetic properties of some synthetic submicron magnetites. Geophysical Journal 94, 83–96.

Maher, B.A., Thompson, R. (Eds.), 1999. Quaternary Climates, Environments and Magnetism. Cambridge University Press, Cambridge, 335pp.

Matzka, J., Maher, B.A., 1999. Magnetic biomonitoring of roadside tree leaves: identification of spatial and temporal variations in vehicle-derived particles. Atmospheric Environment 33, 4565–4569.

Morris, W.A., Versteeg, J.K., Bryant, D.W., Legzdins, A.E., McCarry, B.E., Marvin, C.H., 1995. Preliminary comparisons between mutagenicity and magnetic susceptibility of respirable airborne particle. Atmospheric Environment 29, 3441–3450.

Oldfield, F., 1991. Environmental magnetism – a personal perspective. Quaternary Science Reviews 10, 72–85.

Oldfield, F., Hunt, A., Jones, M.D.H., Chester, R., Dearing, J.A., Olsson, L., Prospero, J.M., 1985. Magnetic differentiation of atmospheric dusts. Nature 317, 516–518.

Oldfield, F., Richardson, N., 1990. Lake sediment magnetism and atmospheric deposition. Philosophical Transactions of the Royal Society of London B 327, 325–330.

Oldfield, F., Thompson, R., Barber, K.E., 1978. Changing atmospheric fallout of magnetic particles recorded in recent ombrotrophic peat sections. Science 199, 679–680.

Ondov, J.M., Ragaini, R.C., Biermann, A.H., 1979. Emissions and particle-size distribution of minor and trace elements at two western coal-fired power plants equipped with coal-side electrostatic precipitators. Environmental Science and Technology 13, 946–953.

Petrovsky, E., Ellwood, B.B., 1999. In: Maher, B.A., Thompson, R. (Eds.), Quaternary Climate, Environment and Magnetism. Cambridge University Press, Cambridge. (Chapter 8).

Pinto, J.P., Stevens, R.K., Willis, R.D., Kellogg, R., Mamane, Y., Novak, J., Santroch, J., Benes, J., Lenicek, J., Bures, V., 1998. Czech air quality monitoring and receptor modelling study. Environmental Science and Technology 32, 843–854.

Shanghai Municipal Environmental Protection Bureau, 1997. Shanghai Environmental Bulletin-1996.

Shu, J., Dearing, J.A., Morse, A.P., Yu, L., Li, C., 2000. Magnetic properties of daily sampled total suspended particles in Shanghai, China. Environmental Science and Technology 34, 2393–2400.

Strzyszcz, Z., 1989. Ferromagnetic properties of forest soils being under the influence of industrial pollution. In: Bucher, J.B., Bucher-Wallin, I. (Eds.), Air Pollution and Forest Decline. 14th International Meeting for specialists in Air Pollution Effects on Forest Ecosystems, IUFRO P2.05, Interlaken, Switzerland, October 2–8, 1998. Birmensdorf, 201.

Thompson, R., 1986. Modelling magnetization data using SIMPLEX. Physics of the Earth and Planetary Interiors 42, 113–127.

Thompson, R., Oldfield, F., 1986. Environmental Magnetism. Allen and Unwin, London (Chapter 11).

Thompson, M., Walsh, J.N., 1991a. In: Trans, F.B., Ying, X. (Eds.), A Handbook of Inductively Coupled Plasma Spectrometry. Metallurgical Industry Press, Beijing (Chapter 9).

Thompson, M., Walsh, J.N., 1991b. In: Trans, F.B., Ying, X. (Eds.), A Handbook of Inductively Coupled Plasma Spectrometry. Metallurgical Industry Press, Beijing, Appendix 2.

Walden, J., Oldfield, F., Smith, J.P. (Eds.), 1999. Environmental Magnetism: a Practical Guide. Technical Guide, No. 6 Quaternary Research Association, London, pp. 35–62.

Wang, M., 1985. Source identification and apportionment for atmospheric aerosol through the application of factor analysis. Scientia Atmospherica Sinica 9, 73–81 (Chinese version).

Watson, J.G., Chow, J.C., 1991. Chemical mass balance. In: Hopke, P.K. (Ed.), Receptor Modeling for Air Quality Management. Elsevier, New York, 1991.

Watson, J.G., Robinson, N.F., Chow, J.C., Henry, R.C., Kim, B.M., Pace, T.G., Meyer, E.L., Nguyen, Q., 1990. The USEPA/DRI Chemical mass balance receptor model CMB 7.0. Environment Software 5, 38–49.

Xie, S., Dearing, J.A., Bloemendal, J., 1999a. A partial susceptibility approach to analysing the magnetic properties of environmental materials: a case study. Geophysical Journal International 138, 851–856.

Xie, S., Dearing, J.A., Bloemendal, J., 1999b. Association between the organic matter content and magnetic properties in street dust, Liverpool, UK. Science of the Total Environment 241, 205–214.

Xudong, H., Ilhan, O., Namic, K.A., 1994. Emissions of elements from motor vehicles: potential marker elements and source composition profile. Atmospheric Environment 28, 1385–1931.

Zhang, J., Cheng, Z., Wang, W., 1998. Source apportionment on fine particles in atmosphere in Beijing (Chinese version, with English abstract). ACTA Scientiae Circumstantiae 18, 62–67.